
Article:
Wu, X., Wang, M. orcid.org/0000-0001-9752-270X, Shen, J. et al. (3 more authors) (2019) Flexible operation of coal fired power plant integrated with post combustion CO2 capture using model predictive control. International Journal of Greenhouse Gas Control, 82. pp. 138-151. ISSN 1750-5836

https://doi.org/10.1016/j.ijggc.2018.12.004

Flexible Operation of Coal Fired Power Plant Integrated with Post Combustion CO_2 Capture Using Model Predictive Control

Xiao Wu[a,*], Meihong Wang[b,*], Jiong Shen[a], Yiguo Li[a],
Adekola Lawal[c], Kwang Y. Lee[d]

[a]Key laboratory of Energy Thermal Conversion and Control of Ministry of Education , Southeast Univerisity, Nanjing 210096, China
[b]Department of Chemical and Biological Engineering, Univerisity of Sheffield, Sheffield S1 3JD, UK
[c]Process Systems Enterprise Ltd, 26-28 Hammersmith Grove, London W6 7HA, UK
[d]Department of Electrical and Computer Engineering, Baylor University, One Bear Place #97356, Waco, TX 76798-7356, USA

Abstract

The growing demand for CO_2 capture from coal-fired power plant (CFPP) has increased the need to improve the dynamic operability of the integrated power generation-CO_2 capture plant. Nevertheless, high-level operation of the entire system is difficult to achieve due to the strong interactions between the CFPP and post combustion CO_2 capture (PCC) unit. In addition, the control tasks of power generation and CO_2 removal are in conflict, since the operation of both processes requires consuming large amount of steam. For these reasons, this paper develops a model for the integrated CFPP-PCC process and analyzes the dynamic relationships for the key variables within the integrated system. Based on the investigation, a centralized model predictive controller is developed to unify the power generation and PCC processes together, involving the key variables of the two systems and the interactions between them. Three operating modes are then studied for the predictive control system with different focuses on the overall system operation; power generation demand tracking and satisfying the CO_2 capture requirement. The predictive controller can achieve a flexible operation of the integrated CFPP- PCC system and fully exert its functions in power generation and CO_2 reduction.

Keywords: Coal-fired power plant; Solvent-based post-combustion carbon capture; Model predictve control; Dynamic behavior analysis; Flexible operation.

1. Introduction

The global warming and climate change are becoming huge threats to the global economic and social development [1]. CO_2 emission reduction has thus gained increasing attention and been acknowledged as a feasible solution to these issues. According to the 2017 Electricity Information Statistics published by International Energy Agency [2], in 2015, the world gross electricity production was 24,345TWh and 39.3% of which was generated from coal-fired power plants (CFPPs). Several billion tons of CO_2 are released into the atmosphere form these CFPPs every day. For this reason, while vigorously developing renewable energy techniques to advance the adjustment of power infrastructure and improving the operating efficiency of CFPPs to reduce their carbon emission intensity, CO_2 capture of CFPPs has been established as a key alternative in reducing the carbon emission and achieving the 2°C global warming control objective in the future 30 years [3].

Post-combustion CO_2 capture (PCC) using chemical solvent such as monoethanolamine (MEA) solution is currently the most mature and promising carbon capture technology for CFPPs. From small pilot-scale plant with a daily capture capacity of several tons [4] to large industrial and commercial-scale plant with daily capture capacity up to several thousand tons [5], the PCC technology has gained much attention and applications in the power industry.

An important factor that restricts the widespread use of PCC technology is the huge heat consumption that is required for solvent regeneration. To this end, developing a simulation model and carrying out simulation studies to find more efficient chemical solvents, process design and operating parameters are the focus of current research.

Cifre et al. [6] presented static models for 600MWe and 1000MWe CFPPs integrated with CO_2 capture and compression devices. The energy impact of PCC process on the power generation was then investigated. The absorber/stripper heights, solvent circulation rate, absorber/stripper temperature/pressure and other design/operating parameters were optimized to attain better

* Corresponding author.
E-mail address: wux@seu.edu.cn (X. Wu); Meihong.Wang@sheffield.ac.uk (M. Wang)

operating efficiency.

To understand the overall performance of the CFPP-PCC integrated system, Aroonwilas and Veawab [7] developed a static 500MWe CFPP-PCC plant model and analyzed the influence of CO_2 capture rate, coal quality, flue-gas delivery mode, solvent selection and re-boiler pressure on the power generation and CO_2 capture processes. In a way similar to the work in [7], Sanpasertparnich et al. [8] conducted simulations on an 800MWe supercritical CFPP-PCC system model. They investigated the performance of the entire plant under different coal grade and re-boiler steam parameters. The work highlighted on the energy consumptions of the PCC plant at different loading conditions: at lower loading conditions, the energy consumptions are relatively higher.

In addition to parameter optimization and process modification, advanced integration options between power plant and CO_2 capture plant were proposed in Oh, Yun and Kim [9], Pan et al. [10] and Wang et al. [11] to improve the net efficiency of the integrated plant. Lucquiaud, Chalmers, and Gibbins [12] analyzed three retrofit options for steam extraction of PCC unit through simulations. The options of Throttled LP Turbine and Floating IP/LP Crossover Pressure were shown to have lower energy consumption. Moreover, flexible adjustment of the extracted steam flow rate was easily attained by these two options. Fernandez et al. [13] also found that the power generation penalty from carbon capture rises when the CFPP is operating at partial load condition. Flexible adjustment of the key parameters in CFPP-PCC system using advanced operation mode was suggested to reduce the cost.

However, these studies were all steady-state analyses undertaken at fixed loading conditions, which completely ignored the dynamics and transient performance of the plant when the operating condition changes. Nevertheless, the CFPP-PCC system has to change frequently the power output and CO_2 capture rate to meet the varying power generation and carbon removal requirements. To understand the dynamic characteristics of the PCC process, dynamic simulations were carried out recently on the first principle models [14], [15] and data-driven identified models [16], [17], where they investigated the dynamic responses of PCC process corresponding to solvent circulation rate, re-boiler heat duty, flue-gas flow rate and composition changes. Faber et al. [18] and Bui et al. [19] conducted experimental studies on pilot PCC plants through open-loop step response tests. Their results revealed the dynamic relationships among the key variables of the PCC process and showed that significant transient time is required for the whole process to enter a new steady state.

To provide guidance for control design over a wide operating range, Wu et al. [20] analyzed the dynamics of PCC process under various working conditions. Their research indicated that under higher capture rate and flue-gas flow rate conditions, the response speed of the PCC process is faster. Moreover, near the optimal re-boiler temperature point, the dynamic variation of the PCC process is significant. Based on the in-depth understanding of the system dynamics, a series of control strategies were proposed for the PCC process. Four key variables were involved in most of these studies, which are CO_2 capture rate, re-boiler temperature, lean solvent flow rate and re-boiler heat duty, because they are highly coupled and reflect the operation performance of the whole PCC process [20]-[27].

The conventional PI/PID based single-loop feedback control designs are the most common approaches [21]-[24]. To attain a quick regulation for the CO_2 capture rate, a typical control loop design is employed, which uses the lean solvent flow rate to control the capture rate and selects the re-boiler heat duty to maintain the re-boiler temperature. Lin et al. [22] proposed to fix the lean solvent flow rate, and instead, control the CO_2 capture rate through adjusting the steam flow rate to re-boiler to change the lean solvent loading. The advantage of this design is that, better hydraulic stability of the absorber and stripper columns is achieved.

To implement more flexible operating condition changes for the PCC process, the model predictive control (MPC) approach has been greatly promoted recently [20], [25]-[28]. By using an explicit process model to predict the future system outputs corresponding to different inputs, the control sequence that yields the most desired output can be obtained by the MPC optimization. Since the MPC can effectively handle the unique characteristics of slow responses, strong couplings and strict constraints of the PCC process, faster capture rate tracking and smaller re-boiler temperature fluctuation performance was achieved in these studies.

Lawal et al. [29] and Posch and Haider [30] proposed to maintain the liquid/gas (L/G) ratio of PCC process to better respond to the flue-gas flow rate change by directly adjusting the lean solvent flow rate. Accurate lean solvent loading or re-boiler temperature control is the prerequisite for the effective use of this approach. In [20], [25], [26], the dynamic influence of flue-gas

flow rate was taken into account in the prediction model development, thus proper lean solvent and re-boiler steam flow rates can be calculated by the MPC in the presence of flue-gas flow rate change.

Although the influence of flue-gas changes was considered in some control designs or performance tests, the conversion process from raw coal to flue gas at the CFPP side was not considered in these studies. Moreover, the dynamic impact of the steam flow to re-boiler on the power generation of the CFPP was not taken into account. Therefore, these dynamic studies were only limited to the independent PCC systems, and the control of the integrated CFPP-PCC system was hardly studied.

For the overall PCC-CFPP system, its control objectives and operating characteristics are more complicated than the individual systems:

1) Both power generation and carbon capture require the steam generated by boilers, which are two desirable but competing tasks. The operation of the integrated CFPP-PCC system must be able to distribute the steam appropriately and timely to meet the changing power generation and carbon capture needs;

2) There are strong interactions between the CFPP and PCC systems. The CFPP has to change its power generation rapidly to meet the varying load requirements of power grid. During the load variation, the flue-gas flow rate change will bring in significant influence on the PCC system operation. On the other hand, the variation of re-boiler steam in the PCC, which is drawn-off from the turbine, will change the power generation and influence the operation of CFPP system; and

3) The integration of CFPP and PCC systems increases the complexity of the overall plant, and control challenges such as coupling, inertia and time delay become more significant.

In Manaf, Qadir and Abbas [31], a hierarchical control structure was proposed for optimal operation of the CFPP-PCC plant. At the upper level, economic optimization was performed to maximize the revenue of the integrated plant, in which the changing electricity price and carbon price were considered and the optimal CO_2 capture rate value was calculated. In the lower level, an MPC was developed for the PCC plant to track the desired capture rate. Mac Dowell and Shah [32] evaluated the economic performance of CFPP-PCC plant in case of load demand and electricity price changes. Four distinct operation scenarios were considered, which were load following, solvent storage, exhaust gas by-pass and time-varying solvent regeneration. It was found that the time-varying solvent regeneration scenario have the best improvement in profit. However, these two studies still focused on the operation of the individual carbon capture system. The dynamics of the CFPP and the integrated operation of the overall CFPP-PCC system were not considered.

In Lawal et al. [33], a 500MWe CFPP-PCC dynamic model was developed using gPROMS, and steady-state optimization was performed for equipment design and solvent selection. In addition to this, simplified decentralized controllers were designed for the CFPP and PCC systems, and two dynamic simulations for reduction of target power output and increase of target CO_2 capture rate were carried out. The results revealed the different responses of the two plants and showed that poor control scheme can have negative effect on the operation of the integrated system.

Olaleye et al. [34] tested the steam reduction/stop strategy in improving the power output adjustment speed on a 600MWe supercritical CFPP-PCC model. The steam to re-boiler drawn-off from the turbine was decreased or stopped temporarily to quickly generate more power to meet the urgent power demand of the power grid. The simulation results showed that about 4.67% the maximum power of the CFPP can be quickly produced by the stripper stop mechanism, which has potential benefit for the wide-range load varying operation of the power plant.

However, the coal pulverizing system, which reflects the key dynamics of the modern CFPP, was not included in the model development of these studies. The models therefore could not fully describe the dynamic process from raw coal to flue gas. Moreover, simplified decentralized PI controllers were used for the complex CFPP-PCC plant, which could not comprehensively handle the interactions between the two systems and were difficult to meet the requirements of the integrated operation.

Given these reasons, this paper develops a CFPP-PCC model to investigate the dynamic relationships among the key variables within the integrated CFPP-PCC system. A centralized MPC is then designed to link the two systems together, estimate and utilize the interactions between them, and achieve a coordinated control of the integrated CFPP-PCC plant. Three operating modes are studied for the MPC, focusing on different targets: overall system operation, rapid power generation demand tracking and strictly satisfying the CO_2 capture requirement. The MPC can greatly benefit the flexible operation of the overall CFPP-PCC system and maximize its functions in power generation and CO_2 reduction.

The following of this paper is organized as follows: Section 2 introduces the integrated CFPP-PCC model and analyzes the

dynamic performance of the overall system. Section 3 presents the centralized MPC design for the integrated CFPP-PCC plant under three operation modes and the simulation results are shown in Section 4. Finally, the conclusions are drawn in Section 5.

2. System Description

2.1 Brief introduction of the PCC model

In [21], a dynamic PCC process was developed based on the design and experimental data of a pilot-scale plant presented in [35]. The model used 30wt% monoethanolamine (MEA) as the absorption solvent and is designed to treat the CFPP flue gas with 0.13kg/s flow rate, 25.2wt% CO_2 concentration under nominal condition. To provide high-fidelity description of the carbon capture process, the model is configured in gCCS environment as shown in Fig. 1 and used as the PCC model in this paper.

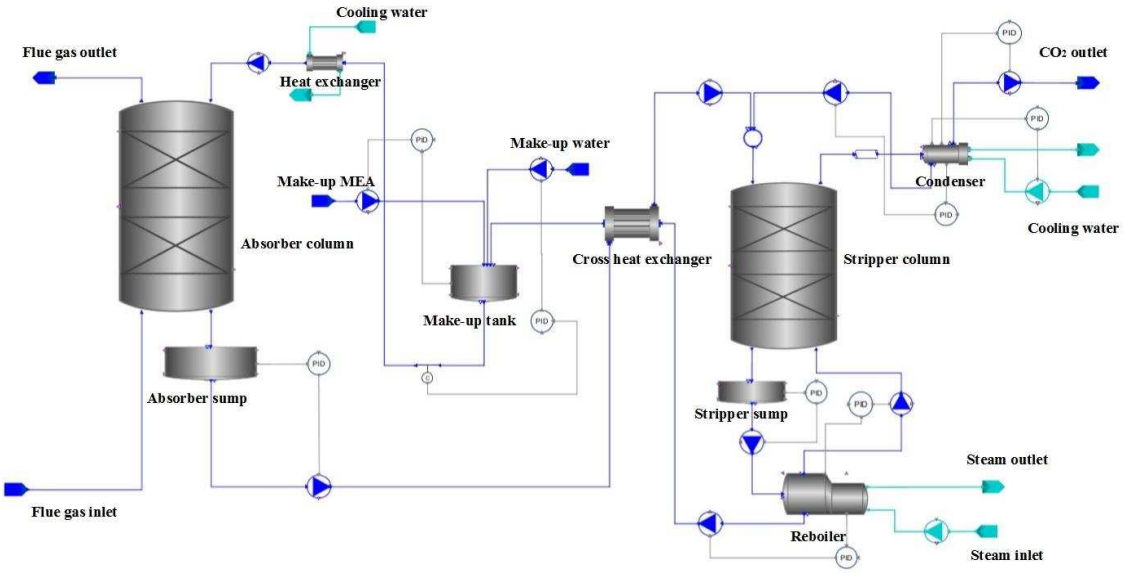

Fig.1. Schematic diagram of solvent-based PCC process developed on the gCCS platform.

2.2 CFPP model development

To study the dynamics of the integrated CFPP-PCC system, a small-scale CFPP model matched with the PCC model has to be developed. The CFPP is a complex multi-variable system, where the most concerned variables in the design framework are the power output and main steam pressure. Generating power is the primary task for the operation of CFPP; and the main-steam pressure indicates the balance between the steam supply of boiler and steam consumption of turbine. Regarding to this, these two variables as well as the corresponding manipulated variables, the coal flow rate command and turbine governor valve, represent the so called boiler-turbine system and is viewed as the top layer of the CFPP control system [36]. For the integration of CFPP and PCC, the coal flow rate command will affect the amount of pulverized coal entering into the boiler and finally determine the flue-gas flow rate on one hand; and on the other hand, the steam to re-boiler of PCC is drawn-off from the crossover of IP/LP turbine, which will influence the power generation of the CFPP. Therefore, description of the dynamics of boiler-turbine unit is the key to the CFPP system modeling. For subsystems with weak couplings, such as the superheater/reheater steam temperature, drum water level, furnace pressure, feedwater temperature etc., we assume that they are well maintained at fixed value by independent local controllers.

In the paper by Lawal et al. [33], a CFPP model was developed without considering the coal pulverizing system. In most of the modern CFPPs, boilers are equipped with direct-firing pulverizing system, in which the coal flow rate command is received as the control signal, and the crushed coal lumps of several cm in diameter are ground to very fine powder (50–100 um in diameter) and sent into the furnace. This process is much slower compared to the dynamics of combustion, mass flow and heat transfer in the boiler. Therefore, the coal pulverizing system reflects the main dynamics in the fuel-air-flue gas passage and have to be considered in the CFPP modeling [37], [38].

A. Coal pulverizing system dynamics

Consider the coal flow rate command q_{cd} as the input of the coal pulverizing system, the flow rate of raw coal entering the mill q_{rc} can be expressed by the pure delay of the coal feeder:

$$q_{rc} = q_{cd} e^{-\tau s} \tag{1}$$

where τ is the delay time.

The mass balance of coal inside the mill is given as:

$$\frac{dm_c}{dt} = q_{rc} - q_{pc} \tag{2}$$

where m_c is the mass of coal stored in the mill and q_{pc} is the flow rate of pulverized coal sent into the furnace.

According to the characteristics of the mill and the pulverized coal separator,

$$q_{pc} = K_1 m_c \tag{3}$$

where pulverizing coefficient K_1 depends on the properties of mill and coal, and varies slightly with the power load.

Since the dynamics of combustion, mass flow and heat transfer in the boiler is much quicker than the coal pulverizing process, we omit these parts of dynamics and consider them together in equations (1) and (2).

Suppose the component of coal and the excessive air ratio of the air supply system are fixed, the effective heat absorbed in the boiler Q_e and flue gas flow rate q_f are proportional to q_{pc}:

$$Q_e = K_2 q_{pc} \tag{4}$$

$$q_f = K_3 q_{pc} \tag{5}$$

where K_2 is the fuel coefficient determined by net calorific value of coal, K_3 is the flue gas coefficient determined by the coal composition and excessive air ratio.

B. Boiler heat storage dynamics

For the boiler, the overall heat balance is given by

$$d(m_{bw}h_{bw} + m_{bs}h_{bs} + m_m c_m T)/dt = Q_e + q_s h_{fw} - q_s h_s \tag{6}$$

where m_{bw} and h_{bw} are the mass and average enthalpy of water in the boiler; m_{bs} and h_{bs} are the mass and average enthalpy of steam in the boiler; m_m, c_m and T are the mass, specific heat capacity and average temperature of metal in the boiler; Q_e is the effective heat absorbed in the boiler; h_{fw} and h_s are the enthalpy of feedwater and generated steam, respectively; q_s is the generated steam mass flow rate fed to the turbine. Because the drum water level is assumed to be well maintained, the mass flow rate of feedwater equals the steam flow rate q_s.

For the drum boiler, the heat stored in the boiler is mainly reflected in the change of the drum pressure p_d, thus equation (6) can be rewritten as:

$$C_b \frac{dp_d}{dt} = Q_e + q_s h_{fw} - q_s h_s \tag{7}$$

$$C_b = m_{bw}\frac{\partial h_{bw}}{\partial p_d} + m_{bs}\partial\frac{h_{bs}}{\partial p_d} + m_m c_m \frac{\partial T}{\partial p_d} \tag{8}$$

where C_b is the boiler heat storage coefficient, which is determined by the boiler type and drum pressure.

C. Pressure drop of superheater

Considering the flow resistance of the superheater pipes, the main steam pressure p_t can be calculated according to the Bernoulli's equation:

$$p_t = p_d - \alpha q_s^2 / \rho_s \tag{9}$$

where ρ_s is the average steam density in the superheater and can be approximated by: $\rho_s = \beta p_d^{1.3}$ according to the property of the superheater steam. Approximate the relationship between Q_e and p_d in (7) as linear, and suppose that the steam flow rate q_s is proportional to the effective heat absorbed in the boiler Q_e, we have:

$$p_t = p_d - K_4 Q_e^{1.3} \tag{10}$$

in which K_4 is the flow resistance coefficient of the superheater.

D. Turbine dynamics

Since the superheater steam temperature is assumed to be fixed, the steam entering into the turbine q_s can be calculated by:

$$q_s = K_5 \mu_t p_t \tag{11}$$

where μ_t is the turbine governor valve opening and K_5 is the valve coefficient.

Then the turbine's power output N can be expressed by:

$$N + K_6 \frac{dN}{dt} = q_s (h_s - h_w) - q_{drawn} (h_{drawn} - h_w) \tag{12}$$

where q_{drawn} and h_{drawn} are the flow rate and enthalpy of the steam to re-boiler drawn-off from the crossover of the IP/LP turbines, K_6 is the time constant of turbine. If all the aforementioned assumptions are satisfied, the enthalpy reduction in the whole turbine, h_s-h_w and in the LP turbine, h_{drawn}-h_w are approximately constant. Suppose the power generated by steam in the LP turbine accounts for 40% of the total power generated in the turbine, i.e., h_{drawn}-h_w =0.4(h_s-h_w), (12) can be further simplified as:

$$N + K_6 \frac{dN}{dt} = (q_s - 0.4 q_{drawn})(h_s - h_w) \tag{13}$$

2.3 Integrated CFPP-PCC model

To connect the CFPP and PCC models together, we assume that: 1) the drawn-off steam from the crossover of IP/LP turbines is first used to heat the feedwater to get depressurized and cooled down to suitable condition before heating the PCC re-boiler; 2) the flue gas is desulfurized, denitrified, dust removed and cooled down to 40 ℃ before being fed into the PCC absorber; and 3) the condensate water of re-boiler steam returns to the CFPP feedwater system.

The process topology of the CFPP-PCC integrated system is presented in Fig. 2. Coal specification for the CFPP is shown in Table 1. Some key operating parameters of the CFPP-PCC system under nominal operating condition are given in Table 2.

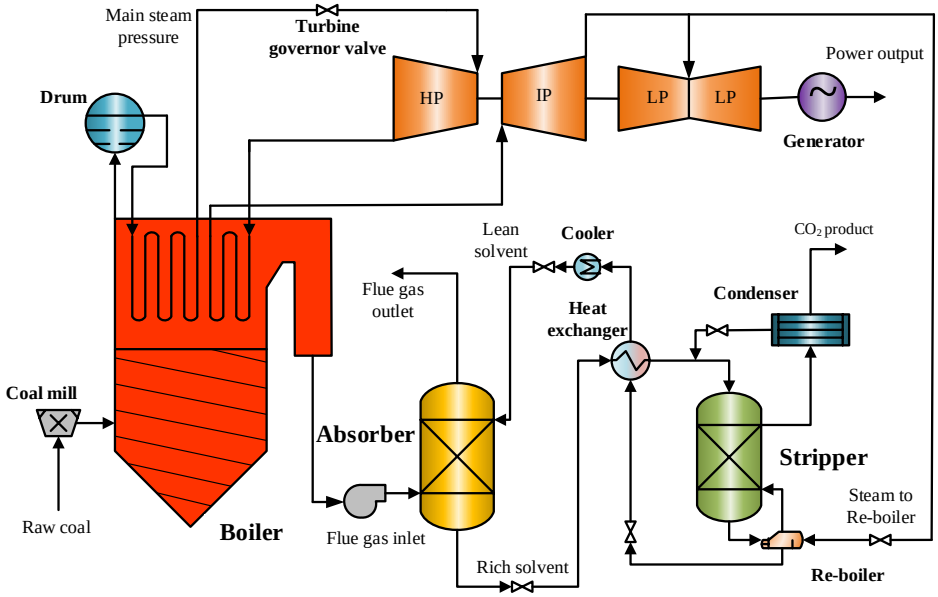

Fig. 2. Process topology of CFPP-PCC integrated system.

Table 1. Coal specification for the CFPP model

Composition	wt% (as received basis)
C	51.93
H	2.36
O	5.88
N	1.42
S	2.07
Moisture	8.92
Ash	27.42

Table 2. Nominal operating condition of key variables for the integrated CFPP-PCC model developed in gCCS

Variable	Unit	Value
Power output	[MWe]	0.176
Turbine governor valve position	[%]	81.09
Coal flow rate command	[kg/s]	0.0234
Drum Pressure	[MPa]	15.41
Main steam pressure	[MPa]	14.76
Excessive air coefficient	/	1.35
Flue gas flow rate	[kg/s]	0.1261
Flue gas CO_2 concentration	[wt%]	25.2
Re-boiler steam flow rate	[kg/s]	0.045
Re-boiler steam pressure	[MPa]	0.3
Re-boiler steam temperature	[K]	410
Flue gas absorber inlet temperature	[K]	313.15
Lean solvent flow rate	[kg/s]	0.5465
MEA concentration	[wt%]	30
Re-boiler pressure	[bar]	1.79
Re-boiler temperature	[K]	386
Condenser Pressure	[bar]	1.69
Condenser temperature	[K]	313.15
CO_2 capture rate*	[%]	90

* CO_2 Capture Rate = $\frac{CO_2 \text{ in the flue gas} - CO_2 \text{ in the clean gas}}{CO_2 \text{ in the flue gas}}$

2.4 Dynamic behavior investigation of the integrated CFPP-PCC system

To study the integrated operation of the CFPP-PCC plant, it is highly important to select related variables and understand the dynamics and interactions among them. As mentioned before, the coal flow rate command, turbine governor valve position, power output and main steam pressure are selected as key variables for the CFPP side. For the PCC process, the lean solvent flow rate, steam flow rate to re-boiler, CO_2 capture rate and re-boiler temperature are selected as the concerned variables, because they indicate the main operating status of the PCC unit and influence the CFPP operation [20]-[27].

The dynamic behavior among these variables are investigated through open-loop step-response tests. We suppose that the CFPP-PCC system is operating at the nominal condition: 0.176MWe power output, 14.7Mpa main steam pressure, 90% CO_2 capture rate and 386K re-boiler temperature point under open-loop condition. At t=5min, step signals in magnitude of -5% of the initial values are added to the manipulated variables (coal flow rate command, turbine governor valve position, lean solvent flow rate and re-boiler steam flow rate) independently. The test results are shown in Figs. 3 and 4.

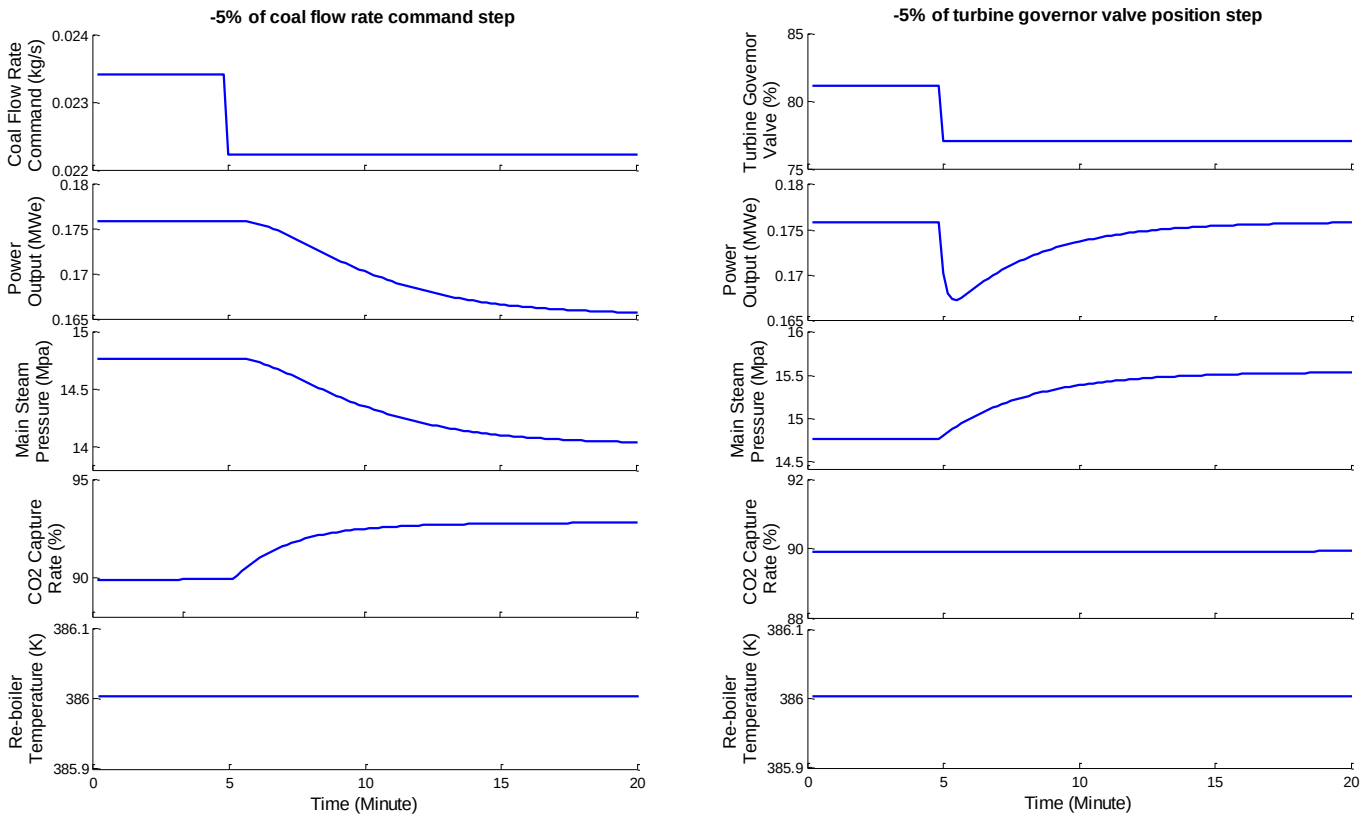

Fig. 3. Responses of the CFPP-PCC integrated system corresponding to -5% coal flow rate command step input (left column) and turbine governor valve step input (right column).

Fig. 3 shows the impact of coal flow rate command and turbine governor valve position on the operation of the CFPP-PCC system. As illustrated in the left column, the reduction of the coal flow command decreases the steam generation in the boiler, which in turn reduces the drum pressure and the main steam pressure. The main pressure reduction then leads to a reduction of the steam flowing into turbine and ultimately reduces the power generation of the CFPP system. The influence of coal flow rate command on the main steam pressure and power output has typical inertial characteristics, the transient process lasts for over 15 min to end the dynamics of coal feeding, pulverizing and delivering into the furnace, and combustion and heat transfer in the boiler. Owing to the same reason, the reduction of coal flow command slowly drops the flue gas flow rate, which then cause a speedy rise of CO_2 capture rate. The capture rate is only increased by 3.22% at steady-state corresponding to 5% reduction of coal flow command, indicating that the amount of captured CO_2 is also decreased and it is difficult to capture the CO_2 in case of lower flue gas flow rate. The re-boiler temperature also slightly rises because the CO_2 loading in rich solvent is decreased. Nevertheless, this impact is very trivial and can be ignored.

As shown in the right column of Fig. 3, the reduction of turbine governor valve position has a speedy influence on the power output because the flow rate of steam flows into the turbine is quickly decreased. However, since the coal flow command remains the same, the heat generated by the boiler remains the same as before. Consequently, the heat stored in water, steam and metal pipes of boiler gradually increases, reflected in the slow rise of the main steam pressure. The power output then returns to the original level. Since the drum boiler has strong heat storage capacity, the whole transient process takes about 10 minutes to enter new steady-state. The turbine governor valve has little impact on the operation of the PCC process.

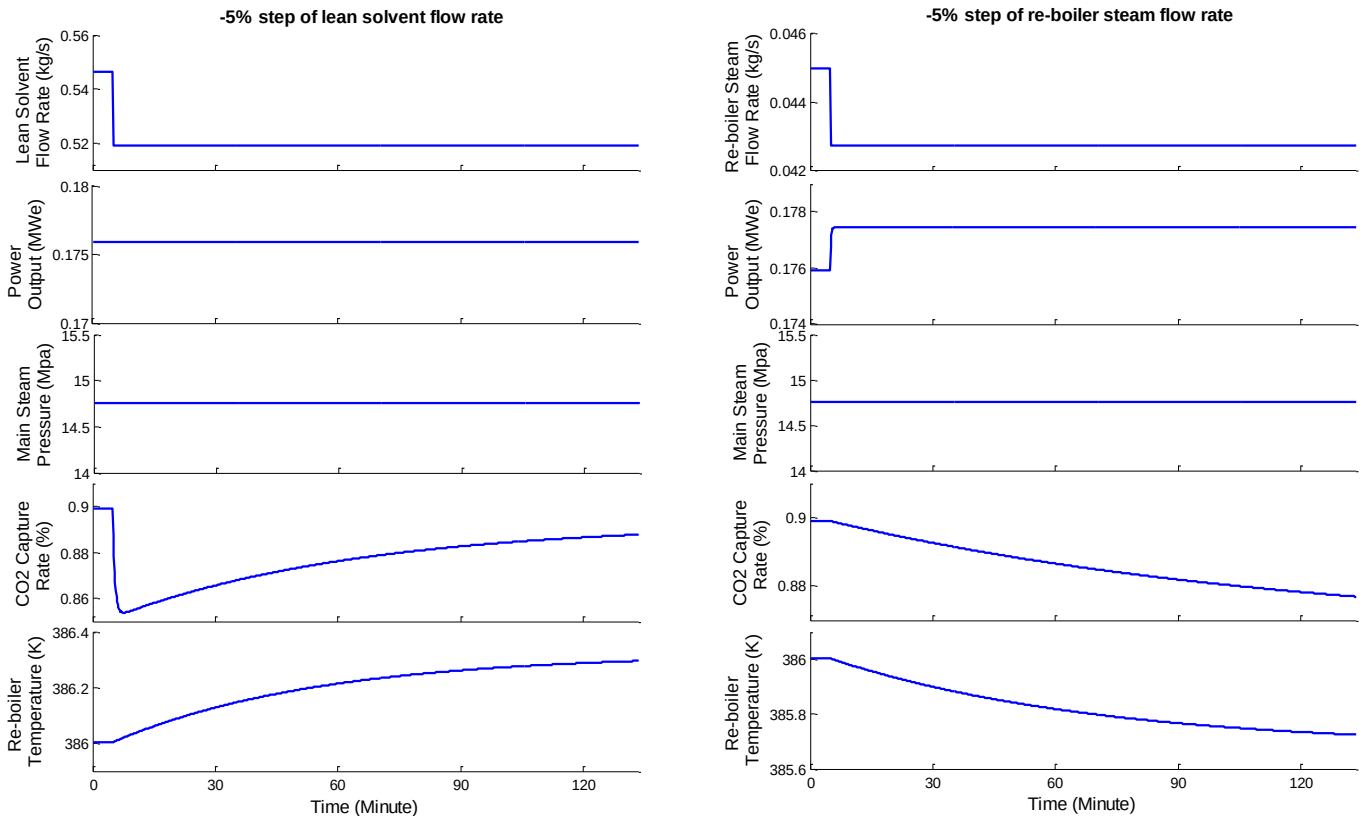

Fig. 4. Responses of the CFPP-PCC integrated system corresponding to -5% lean solvent flow rate step input (left column) and re-boiler steam flow rate step input (right column).

Fig. 4 shows the impact of lean solvent flow rate and re-boiler steam flow rate on the operation of the CFPP-PCC system. As illustrated in the left column, the reduction of lean solvent flow rate has no effect on the CFPP operation. However, for the PCC system, reducing the chemical solvent in direct contact with CO_2 will decrease the CO_2 capture rate quickly in 2-3 min. However, as the rich solvent decreases to flow into the stripper and re-boiler, the unchanged re-boiler heat will slowly raise the re-boiler temperature. Consequently, the lean solvent CO_2 loading will be decreased, strengthening the CO_2 capture ability of the lean solvent; and the capture rate slowly rises back to its original level. The re-boiler temperature takes more than 2 hours to stabilize and the response of the capture rate is even more sluggish.

As shown in the right column of Fig. 4, the reduction of re-boiler steam flow rate has no impact on the main steam pressure of CFPP, but will speedily increase the power output, because more steam will flow into the LP turbine for power generation. As less steam is now used for heating the re-boiler, the re-boiler temperature gradually drops, which increases the CO_2 loading of the lean solvent and finally leads to the reduction of CO_2 capture rate. The responses of the CO_2 capture rate and re-boiler temperature are also very slow corresponding to the re-boiler steam flow rate change.

The step response tests in Figs. 3 and 4 clearly demonstrate the inertial characteristics of the integrated CFPP-PCC system. Moreover, there are strong interactions between the two systems. If these interactions are not considered and effectively handled, significant unknown disturbances will be brought into the controller resulting in poor performance. Moreover, since the power generation and CO_2 capture are two conflicting tasks, these interactions will severely disrupt the integrated operation of the entire system. Take the load ramping-up operation of the CFPP as an example, in order to increase the load, the CFPP controller must increase the coal mass flow command, which will cause an increase for the flue gas flow rate and rapidly drop the CO_2 capture rate of the PCC system. Without effective coordination with the CFPP system, the PCC control will increase the steam flow rate to re-boiler to compensate for the capture rate reduction, which in turn will slow down the load ramping speed of the CFPP.

Therefore, it is important to integrate the CFPP and PCC systems together and develop advanced control scheme to coordinate their operation, so that the power generation and CO_2 emission reduction capabilities of the integrated system can be fully exercised.

3. Coordinated Control Design of the Integrated CFPP-PCC Unit Using Centralized MPC

4.1 Centralized model predictive control design for the CFPP-PCC unit

Developing a centralized multi-variable controller provides the most direct and effective way to consider the interactions among involved variables. Thus, a centralized MPC is devised to link the dynamic behaviors of CFPP and PCC systems together. Owning to the feature of MPC that uses a system model to predict the future outputs of the plant under different input sequences, appropriate input sequence that can generate the most desired future output can be found through optimization. Therefore, the MPC is naturally suited to handle the slow response and strict constraints of the CFPP-PCC system. The structure of the proposed controller is shown in Fig. 5.

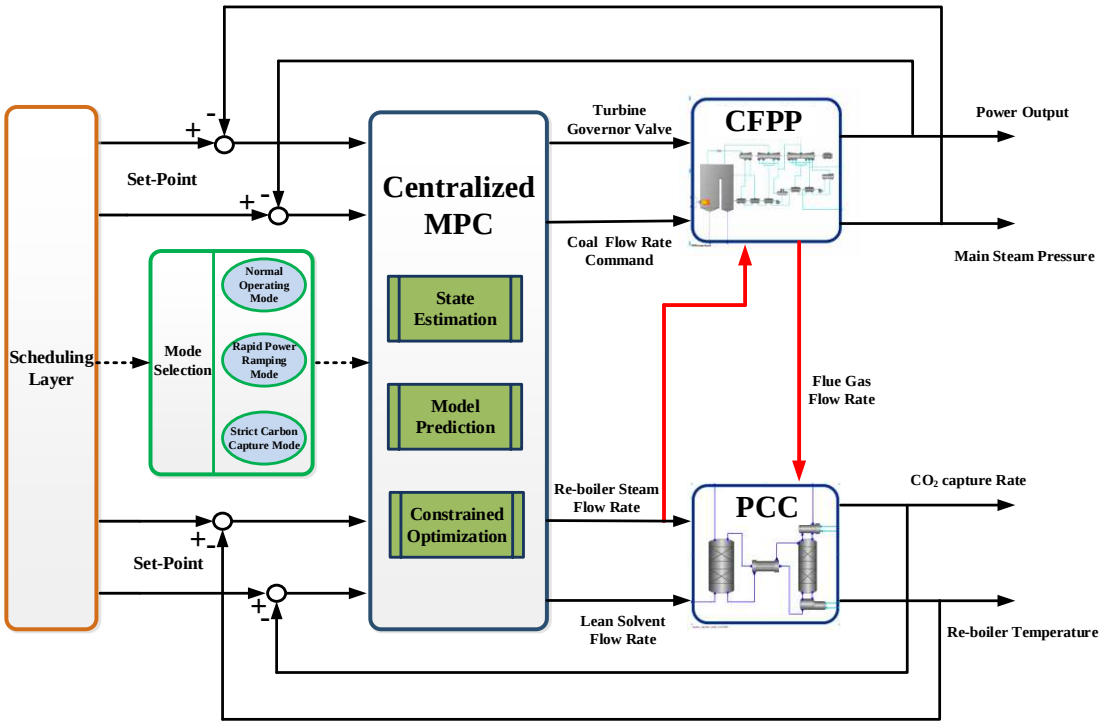

Fig. 5. Schematic diagram of the proposed centralized MPC system structure for the integrated CFPP-PCC system.

To facilitate the design of multivariable controller, the following discrete state-space model is selected as the prediction model:

$$\begin{cases} x_{k+1} = Ax_k + Bu_k \\ y_k = Cx_k + Du_k \end{cases} \tag{14}$$

in which u_k is input vector at time instant k, including coal flow rate command, turbine governor valve position, lean solvent flow rate and re-boiler steam flow rate; y_k is the output vector at time instant k, including power output, main steam pressure, CO_2 capture rate and re-boiler temperature; x_k is the state vector at time instant k; and A, B, C, D are the model matrices, which are determined through an identification technique using the input-output data. The state vector x_k is arbitrarily selected during the identification, thus may not have physical meanings and cannot be measured. Therefore, a state observer is required to estimate its value:

$$\begin{cases} \hat{x}_{k+1} = A\hat{x}_k + Bu_k + F(\hat{y}_k - y_k) \\ \hat{y}_k = C\hat{x}_k + Du_k \end{cases} \tag{15}$$

where the symbol "^" represents the estimation. Following the method given in [39], the observer gain F can be computed if there exist matrices H and G, and a symmetric positive definite matrix X, such that the following Linear Matrix Inequality (LMI) problem is feasible:

$$\begin{bmatrix} H^T + H - X & (HA+GC)^T \\ HA+GC & X \end{bmatrix} > 0 \tag{16}$$

and the observer gain becomes $F=H^{-1}G$.

Stacking up model (15) for N_y steps, future output sequences form a vector $\hat{y}_f = \left[\hat{y}_{k+1}^T \quad \hat{y}_{k+2}^T \quad \cdots \quad \hat{y}_{k+N_y}^T\right]^T$ within the predictive horizon N_y, which can be expressed by future input sequence $u_f = \left[u_{k+1}^T \quad u_{k+2}^T \quad \cdots \quad u_{k+N_u}^T\right]$ defined over a control horizon N_u:

$$\hat{y}_f = \psi_x \hat{x}_k + \psi_u \left[u_f \quad \underbrace{u_{k+N_u}^T \quad \cdots \quad u_{k+N_u}^T}_{(N_y - N_u)\text{items}} \right]^T + \psi_y y_k \tag{17}$$

in which

$$\psi_x = \begin{bmatrix} C \\ CA \\ \vdots \\ CA^{N_y-1} \end{bmatrix} (A + FC), \quad \psi_y = -\begin{bmatrix} C \\ CA \\ \vdots \\ CA^{N_y-1} \end{bmatrix} F,$$

$$\psi_u = \begin{bmatrix} C(B+FD) & D & 0 & \cdots & 0 \\ CA(B+FD) & CB & D & 0 & 0 \\ \vdots & \vdots & \vdots & \ddots & \vdots \\ CA^{N_u-1}(B+FD) & CA^{N_u-2}B & \cdots & CB & D \\ CA^{N_u}(B+FD) & CA^{N_u-1}B & \cdots & CAB & CB+D \\ \vdots & \vdots & \vdots & \vdots & \vdots \\ CA^{N_y-1}(B+KD) & CA^{N_y-2}B & \cdots & CA^{N_y-N_u}B & \sum_{j=0}^{N_y-N_u-1} CA^j B + D \end{bmatrix}$$

Here, we have assumed that the control horizon N_u is shorter than the predictive horizon N_y, and the future control actions beyond N_u remains the same.

Considering the dynamic behavior of the integrated CFPP-PCC unit as shown in Figs. 3 and 4, the fastest dynamics of the process come from the responses of power output corresponding to the changes of turbine governor valve position and steam flow rate to re-boiler (around 30s to reach the peak values). The lean solvent flow rate also has a speedy influence on the CO_2 capture rate at early stage (around 150s to reach the peak values). In order to capture these key dynamic properties of the CFPP-PCC process, the sampling time of the predictive model is set as 30s. Selecting excessively smaller sampling times will catch too much system noise and increase the computational complexity of the controller.

The predictive horizon N_y is set as 40 steps, so that the CFPP-PCC system's response in future 1200s can be made by the MPC. Although the entire transient process of the PCC system takes more than 2 hours to finish, this prediction time can cover the main features and trends of the system response. In addition, this will not cause too much computational burden for the controller. The control horizon N_u is then set as 5 steps to further reduce the computational complexity and improve the robustness of the MPC.

To include the integral action into the MPC to compensate for the control offset caused by system dynamic changes or modeling mismatches, an incremental type of model prediction is used in the MPC design [40]:

$$\Delta\hat{y}_f = \psi_x \Delta\hat{x}_k + \psi_u \left[\Delta u_f \quad \underbrace{0_{1\times4} \quad \cdots \quad 0_{1\times4}}_{(N_y - N_u)\text{items}} \right]^T + \psi_y \Delta y_k \tag{18}$$

where $\Delta\hat{y}_f$ is the future incremental output sequence $\Delta\hat{y}_f = \left[\Delta\hat{y}_{k+1}^T \quad \Delta\hat{y}_{k+2}^T \quad \cdots \quad \Delta\hat{y}_{k+N_y}^T\right]^T$; Δu_f is the future incremental input sequence $\Delta u_f = \left[\Delta u_{k+1}^T \quad \Delta u_{k+2}^T \quad \cdots \quad \Delta u_{k+N_u}^T\right]^T$; $\Delta\hat{x}_k$, Δu_k and Δy_k are the incremental values of the estimated state, input and output vectors at time k, $\Delta x_k = x_k - x_{k-1}$, $\Delta u_k = u_k - u_{k-1}$, $\Delta y_k = y_k - y_{k-1}$.

Then, we can have

$$\hat{y}_f = \begin{bmatrix} y_k \\ y_k \\ \vdots \\ y_k \end{bmatrix} + \begin{bmatrix} I_4 & 0_4 & \cdots & 0_4 \\ I_4 & I_4 & \cdots & 0_4 \\ \vdots & \vdots & \ddots & \vdots \\ I_4 & I_4 & \cdots & I_4 \end{bmatrix} \Delta\hat{y}_f \tag{19}$$

Equation (19), together with (18), expresses the future output of the CFPP-PCC system as a function of future input. Based on this, appropriate input sequence that can generate the desired future output can be selected.

The following dynamic objective function is used to evaluate the performance of the input sequence:

$$J = (\hat{y}_f - r_f)^T Q_f (\hat{y}_f - r_f) + \Delta u_f^T R_f \Delta u_f \tag{20}$$

where $r_f = \begin{bmatrix} r_{k+1}^T & r_{k+2}^T & \cdots & r_{k+N_y}^T \end{bmatrix}^T$ is the future set-points for the controlled variables. The first item in objective function (20) represents the set-point tracking performance of the MPC. Sluggish tracking of the set-point is not desirable, thus corresponds to a larger objective function value. $Q_f = I_{N_f} \otimes Q_0$ is the weighting matrix, in which Q_0 is a 4×4 diagonal matrix reflecting the different importance for power output, main steam pressure, CO_2 capture rate and re-boiler temperature adjustment. The second item in (20) represents the smooth regulation performance of MPC. Frequent and strong variation of the input signal is not desirable, since it will influence the stable and safe operation of the plant and may even shorten the service life of the actuators. $R_f = I_{N_u} \otimes R_0$ is the weighting matrix, in which R_0 is a 4×4 diagonal matrix reflecting the different importance for coal flow rate command, turbine governor valve position, lean solvent flow rate and re-boiler steam flow rate variations.

Since the optimal input sequence is computed through minimizing the objective function, the amplitude and rate constraints due to physical limitations of the actuators can be imposed on the input sequence before optimization as following:

$$\begin{bmatrix} I_4 \\ I_4 \\ \vdots \\ I_4 \end{bmatrix} (u_{min} - u_k) \le \begin{bmatrix} I_4 & 0_4 & \cdots & 0_4 \\ I_4 & I_4 & \cdots & 0_4 \\ \vdots & \vdots & \ddots & \vdots \\ I_4 & I_4 & \cdots & I_4 \end{bmatrix} \Delta u_f \le \begin{bmatrix} I_4 \\ I_4 \\ \vdots \\ I_4 \end{bmatrix} (u_{max} - u_k) \tag{21}$$

$$\begin{bmatrix} I_4 \\ I_4 \\ \vdots \\ I_4 \end{bmatrix} \Delta u_{min} \le \Delta u_f \le \begin{bmatrix} I_4 \\ I_4 \\ \vdots \\ I_4 \end{bmatrix} \Delta u_{max} \tag{22}$$

Therefore, at each sampling time, substitute the model prediction (19) into the objective function (20), and minimize (20) subject to the input amplitude and rate constraints (21) and (22), the optimal future incremental control sequence Δu_f can be found. The first element Δu_{k+1} is then extracted to get the control action at the next step: $u_{k+1}=u_k+\Delta u_{k+1}$, which will be implemented on the CFPP-PCC system. This calculation process will be repeated at the next sampling time to achieve a step-by-step receding horizon optimization.

4.2 Three operation modes design for the centralized control of integrated CFPP-PCC plant

To coordinate the integrated operation of the CFPP-PCC plant and better exert its power generation and CO_2 emission reduction functions, three operation modes are presented for the centralized MPC system.

A. Normal operating mode

When operating under the normal mode, the CFPP-PCC system treats the power generation and CO_2 capture tasks equally. The MPC receives the power generation and CO_2 capture rate commands issued by the scheduling layer and optimizes the objective function (20) subject to the constraints (21) and (22), driving the plant to track these commands quickly and smoothly.

Generally, the commands are directly given based on the grid and environmental requirements. In a few cases, if the plant has the right to operate autonomously, the commands can be given by the experienced operators according to their personal preferences or computed through steady-state economic optimizations aiming at maximizing the operating profit of the

CFPP-PCC plant:

$$\begin{aligned} &\min J = -(P_{power} y_1 + P_{co_2} \alpha u_1 y_3 - P_{coal} u_1) \\ &\text{s.t.} \qquad y = f(u) \\ &\qquad\quad y_{min} \le y \le y_{max} \\ &\qquad\quad u_{min} \le u \le u_{max} \end{aligned} \tag{23}$$

in which the P_{power}, P_{CO2}, P_{coal} are the price of electricity, CO_2 and raw coal; y is the output of the CFPP_PCC system, including y_1: power output, y_2: main steam pressure, y_3: CO_2 capture rate, y_4: re-boiler temperature; u is the input of the CFPP_PCC system, including u_1: coal flow rate command, u_2: turbine governor valve position, u_3: lean solvent flow rate, u_4: re-boiler steam flow rate; α is the conversion coefficient between the coal and flue gas mass flow; f is the steady-state model between the input and output; y_{min}, y_{max} and u_{min}, u_{max} are the operating requirements and limitations of the CFPP-PCC unit.

B. Rapid power ramping mode

With the great promotion of renewable power sources such as wind and solar, the CFPPs are required to undertake the grid's peak regulation task and change the power load as fast as possible in a wide operating range, so that the fluctuations caused by the intermittent renewable sources and varying load demand can be compensated in time. Nevertheless, as shown in Fig. 2, the conversion process from raw coal to power generation is slow, and the power adjustment capability of turbine governor valve depends on the heat stored in boiler, which is temporary and limited. Therefore, rapid power change increases the control difficulties of CFPPs.

As illustrated in Fig. 4 for the integrated CFPP-PCC system, adjusting the re-boiler steam flow rate provides a more efficient way to increase the power ramping speed. The change of steam flow rate to re-boiler can quickly change the inlet steam flow rate of the LP turbine and change the power load of the entire unit in around 30s. Such a power load regulation speed is much faster than that of the coal flow rate command.

Therefore, a rapid power ramping mode is proposed in the case of urgent load varying demand and relaxed carbon capture requirement. Under this mode, the MPC receives the power generation instructions from the scheduling layer and makes every effort to improve the power load ramping speed of the CFPP-PCC unit. The steam flow rate to re-boiler is forced to rise/drop at the maximum rate within the constraints until the power output is close to the desired value. Because the re-boiler steam is now used for auxiliary power regulation, the CO_2 capture rate cannot be controlled in this mode. Weights corresponding to capture rate and re-boiler steam flow rate in the weighting matrices Q_0 and R_0 are set as zeros. The MPC tries to adjust the lean solvent flow rate to maintain the re-boiler temperature at the desired level, ensuring safe and economical operation of the PCC system.

C. Strict carbon capture mode

With the growing maturity of PCC technology, in the future, the CFPPs may be required to strictly control their CO_2 capture rate beyond a certain level, following the current requirements on desulfurization and denitrification.

The strict carbon capture mode is proposed for this situation, the MPC receives the power generation set-points from the scheduling layer and drives the plant to track the set-points, meanwhile, maintaining the CO_2 capture rate beyond a given level is of higher importance to meet the goal of carbon emission reduction. Such a control requirement is challenging, because during the power load variation of CFPP, the change of coal mass flow rate will cause the change of flue gas flow rate and bring in significant disturbances on the operation of PCC process.

To ensure a satisfactory CO_2 capture rate control performance and alleviate the influence of varying flue-gas flow rate, weights corresponding to the capture rate and coal flow rate command in the weighting matrices Q_0 and R_0 are enhanced in this mode. In addition, the following soft constraint for CO_2 capture rate control is included in the optimization to ensure the capture rate higher than the requested level during the operation:

$$y_f^{capture\_rate} \ge \begin{bmatrix} 1 \\ 1 \\ \vdots \\ 1 \end{bmatrix} y_{min}^{capture\_rate} - \varepsilon \tag{24}$$

where $y_f^{capture\_rate}$ is the future CO_2 capture rate within the prediction horizon, $y_{min}^{capture\_rate}$ is the lower bound of the capture rate. To guarantee the feasibility of the optimization, a slack vector ε of the positive numbers is added in (24) to soften the constraint. The objective function (20) is then changed to include the penalty for violation of the constraints:

$$J = (\hat{y}_f - r_f)^T Q_f (\hat{y}_f - r_f) + \Delta u_f^T R_f \Delta u_f + \varepsilon^T S_f \varepsilon \quad (25)$$

where S_f is the corresponding weighting matrix.

4. Simulation Results

To demonstrate the advantages of the proposed centralized MPC, dynamic simulations of the integrated CFPP-PCC unit are carried out using different control strategies. The parameters of the MPC under normal operating mode are set as follows: Sampling time T_s=30s, predictive horizon N_y=40, control horizon N_u=5; the output weighting matrix Q_0 is set as Q_0=diag(15000, 2, 5000, 100) for the control of power output, main steam pressure, CO_2 capture rate and re-boiler temperature, respectively, with emphasis on the power output and capture rate adjustment; the input weighting matrix R_0 is set as R_0=diag(4000, 1, 5, 25) for the variation restrictions of coal flow rate command, turbine governor valve position, lean solvent flow rate and steam flow rate to re-boiler, respectively, focusing on avoiding the dramatic changes of coal mass flow rate. Considering the physical limitations of the actuators, input magnitude and rate constraints are given as: $u_{min}=[0.01, 50, 0.2, 0.05]^T$, $u_{max}=[0.029, 90, 1, 0.08]^T$; $\Delta u_{min}=[-0.001, -5, -0.0035, -0.0005]^T$, $\Delta u_{max}=[0.001, 5, 0.0035, 0.0005]^T$.

Case 1: The first simulation is designed to test the overall performance of the proposed MPC under normal operating mode. The power output and CO_2 capture rate set-points are changed simultaneously in this case and tracking of them is the task of the controllers. We assume that in the beginning of the simulation, the CFPP-PCC system is operating at 0.2MWe power output, 15.88MPa main steam pressure, 75% CO_2 capture rate and 386K re-boiler temperature condition. At t=10min, new set-points are issued by the scheduling layer that, the power output and CO_2 capture rate set-points change to 0.13MWe and 90%, respectively; then at t=60min, the power output and CO_2 capture rate set-points change to 0.225MWe and 50%, respectively. The CFPP is operating at the sliding pressure mode, thus the main steam pressure set-point changes to 13.60 MPa and 16.38MPa accordingly. The re-boiler temperature set-point remains the same at 386K, which is the economical temperature for the operation of the PCC unit.

Besides the proposed centralized MPC, two other controllers are used for comparison, which are:

A. Independent MPCs: Two independent MPCs are designed for each of the CFPP and PCC. The MPC for the CFPP (MPC_CFPP) uses coal flow rate and turbine governor-valve position as commands to regulate the power output and main steam pressure. The steam drawn-off to the re-boiler is not considered in the MPC design; and the MPC for the PCC (MPC_PCC) uses the lean solvent flow rate and re-boiler steam flow rate to control the CO_2 capture rate and re-boiler temperature. The flue-gas flow rate variation is not considered and is fixed at 0.13kg/s in the MPC design. The parameters of the two independent MPCs are set the same as those in the centralized MPC.

B. Decentralized PI controllers: Four proportional-integral (PI) controllers are designed for the combined CFPP-PCC process, where boiler following mode (using turbine governor valve to adjust the power output, coal mass flow rate to adjust the main steam pressure) is used to design PI controllers for the CFPP (PI_CFPP) to achieve a rapid tracking of power demand. To design PI controllers for the PCC (PI_PCC), the lean solvent flow rate is adopted to regulate the capture rate, and the steam flow rate to re-boiler is adopted to regulate the re-boiler temperature. The controller gains of the four PIs are set as follows:

Power control loop: K_P=30, K_I=0.8;

Main steam pressure control loop: K_P =0.0004, K_I =0.00004;

CO_2 capture rate control loop: K_P = 0.006, K_I = 0.0015;

Re-boiler temperature control loop: K_P =0.07, K_I =0.0008;

The simulation results are shown in Fig. 6. They indicate that speedy and smooth control of the integrated CFPP-PCC plant can be achieved by the proposed centralized MPC. It only takes around 11 minutes to track the new power load demands and 9 minutes to track the new capture rate demands, and the overshoots of these two key variables during the adjustment are trivial. Meanwhile, the main steam pressure can follow the set-point variation in time and re-boiler temperature is tightly maintained

around 386K.

When the power load demand drops in a wide range, the load tracking task is mainly attained by decrease the coal flow rate command and turbine governor valve position. In the early stage of regulation, the re-boiler steam flow rate is increased to accelerate the power load change speed and enhance the rising rate of CO_2 capture rate. However, continuing the speedy decrease of coal flow rate will cause strong growth of the capture rate, which may lead a serious overshoot. Thus, after a short time of the increase, the lean solvent flow rate and re-boiler steam flow rate are decreased in advance to compensate for the reduction in coal flow rate and attain a satisfactory CO_2 capture rate. During the adjustment process, the changes of lean solvent flow rate and re-boiler steam flow rate are kept consistent with each other to maintain the re-boiler temperature. The control actions for power load rising and capture rate reduction are almost the same. The difference is that, for the large CO_2 capture rate change from 90% to 50%, the decline in lean solvent and re-boiler steam flow rates continues for a longer period to achieve faster capture rate adjustment. Because the CFPP and PCC systems are regarded as an integrated unit in the centralized MPC design, the interactions among variables in the two systems can be fully considered during the operation. Coordinated control of the entire CFPP-PCC unit has been successfully achieved in normal operating mode.

Regarding the independent MPCs, the variations of coal flow rate and re-boiler steam flow rate reduce the accuracy of model predictions and degrade their control performance. The tracking speed of power output and CO_2 capture rate is significantly slower than the proposed centralized MPC, with large overshoot during the regulation process. Moreover, because the interactions between CFPP and PCC systems are not taken into account in controller design, the coal flow rate and re-boiler steam flow rate variations bring in severe unknown disturbances into the PCC and CFPP controllers and deteriorate the smooth operation of the two systems. Strong fluctuations in all the four MVs can be viewed clearly in Fig. 6 for the independent MPCs. The frequent variation of the MVs will shorten the service life of actuators and endanger the safety of the plant.

For the decentralized PI controllers, sluggish responses of the power output, main steam pressure and CO_2 capture rate are observed in Fig. 6. Although the trend of adjustment is reasonable, it is challenging for the past error-based PI control to meet the prompt regulation requirement of slow CFPP-PCC plant. Moreover, the single-loop based PI controller cannot consider the interactions among multi-loops and calculate the best control input in the presence of constraints.

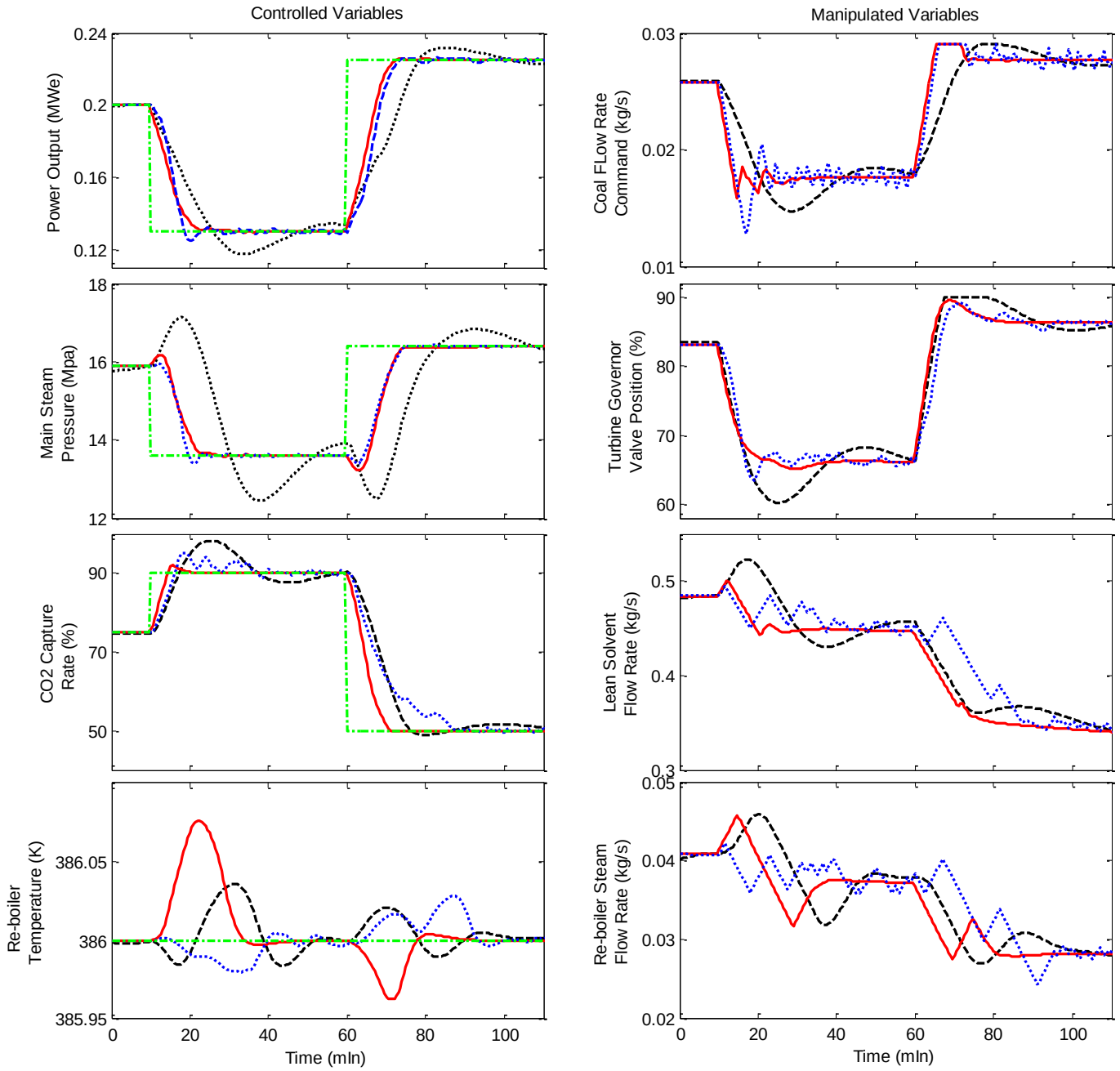

Fig. 6. Performance of the integrated CFPP-PCC system in Case 1: left column: controlled variables; right column: manipulated variables (solid in red: proposed centralized MPC; dotted in blue: independent MPCs; dashed in black: decentralized PI controllers; dot-dashed in green: reference).

Case 2: The second case is designed to verify the performance of the centralized MPC in situation that fast regulation of power generation is required. We suppose that in the beginning of the simulation, the CFPP-PCC unit is operating at 0.145MWe power output, 13.80MPa main steam pressure, 90% CO_2 capture rate and 386K re-boiler temperature condition. At t=10min and t=60min, the power load demand changes to 0.2MWe and 0.16MWe, respectively, and due to the requirement of power grid's peak regulation, tracking the power load demand is the most urgent task. The main steam pressure set-point changes to 15.88MPa and 14.02MPa according to the power demand changes under the sliding pressure mode; and the CO_2 capture rate and re-boiler temperature set-point remains the same in this case.

The proposed centralized MPC under rapid power ramping mode is used to test the regulation task. To demonstrate its advantages in power load variation, it is compared with the same centralized MPC designed under normal operating mode and another MPC designed only for the CFPP unit. The simulation results are shown in Fig. 7.

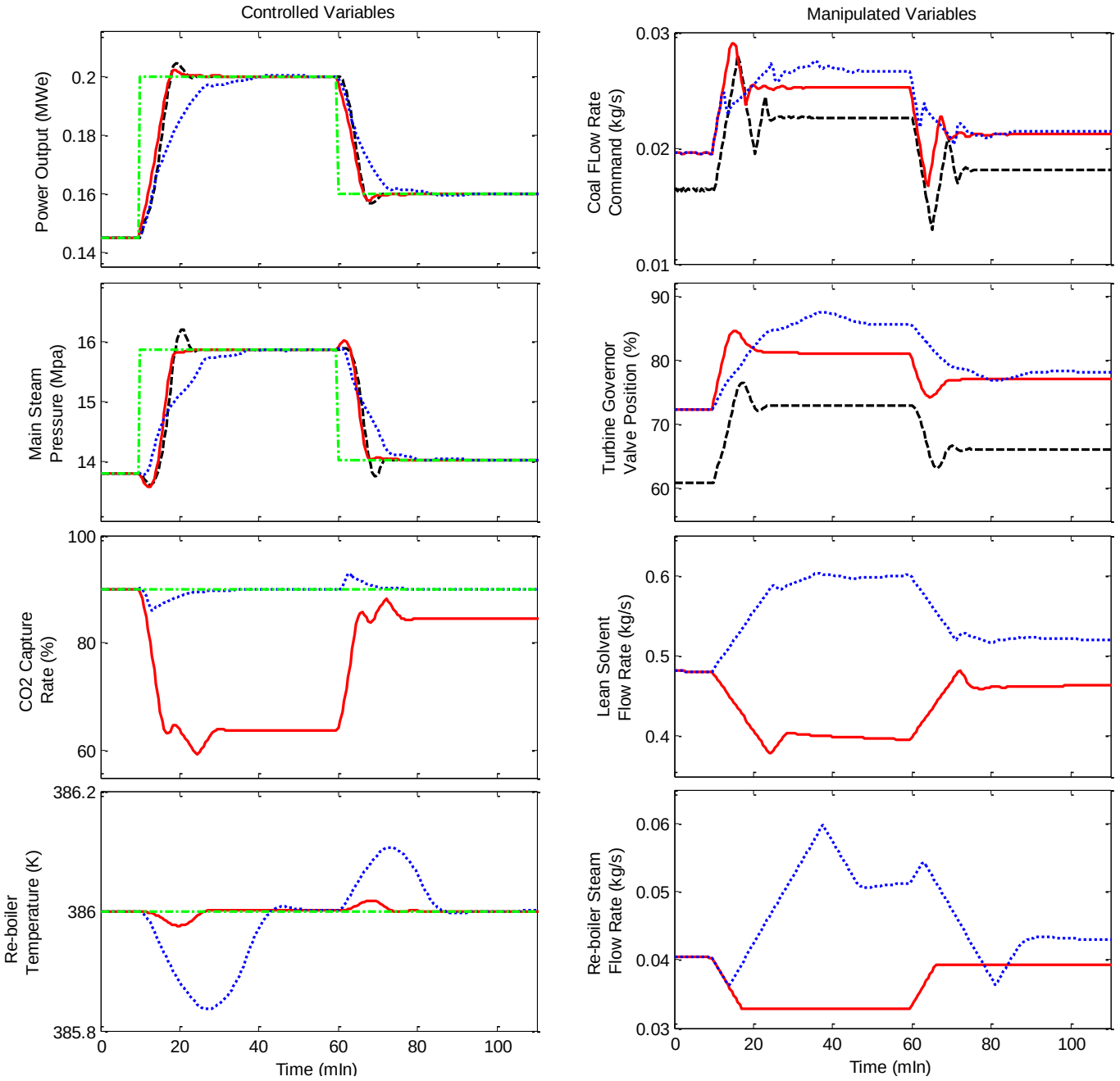

Fig. 7. Performance of the integrated CFPP-PCC system in Case2: left column: controlled variables; right column: manipulated variables (solid in red: proposed centralized MPC under rapid power ramping mode; dotted in blue: proposed centralized MPC under normal operating mode; dashed in black: conventional MPC of an individual CFPP unit; dot-dashed in green: reference).

The results show that the proposed centralized MPC under rapid power ramping mode has the fastest power load tracking speed. Take the power load increase process as an example, when the power command rises, the coal flow rate and turbine governor valve are increased to provide more steam for the turbine, moreover, the re-boiler steam flow rate is speedily decreased, so that the steam originally used for solvent regeneration can continue to expand in the LP turbine and generate more power. With the re-boiler steam assisted power load regulation, the power increase task is completed within 8 minutes and the biggest overshoot is only 0.0021MWe. Since the power load becomes simpler to control, the actions of the turbine governor valve and coal flow rate command can pay more attention to the main steam pressure control and better steam pressure control can be observed under this mode.

Note that with the help of re-boiler steam auxiliary adjustment, the power and pressure control performance of the integrated CFPP-PCC plant is even better than that of the independent CFPP: the transient process is about 1 minute shorter and the control overshoot is much smaller. The advantages of CFPP-PCC system in power load regulation is clearly demonstrated in this

simulation.

The expense of rapid power load change is the loss of CO_2 capture rate adjustment. Because the re-boiler steam flow is used as an additional means to regulate the power, the CO_2 capture rate can no longer be maintained at the given level. To guarantee a safe and optimal operation of the PCC process under this mode, the lean solvent flow rate is regulated in response to the variation of re-boiler steam flow rate and coal flow rate command in order to maintain the re-boiler temperature. As shown in Fig. 7, the re-boiler temperature can be controlled closely around 386K.

For the proposed centralized MPC under normal operating mode, the actions of coal flow rate command and re-boiler steam flow rate are similar to the rapid power ramping mode at the early stage of regulation to ensure a fast increase of the power load. However, considering the requirement for CO_2 capture rate control, the increased speed of coal flow rate command is slowed down and the steam flow rate to re-boiler begins to rise soon. The rate of change in turbine governor valve is also reduced to avoid strong deviation in the main steam pressure control. As a result, the power load increase/decrease process respectively takes 28/21 minutes to complete, which is much slower than that of the rapid power ramping mode.

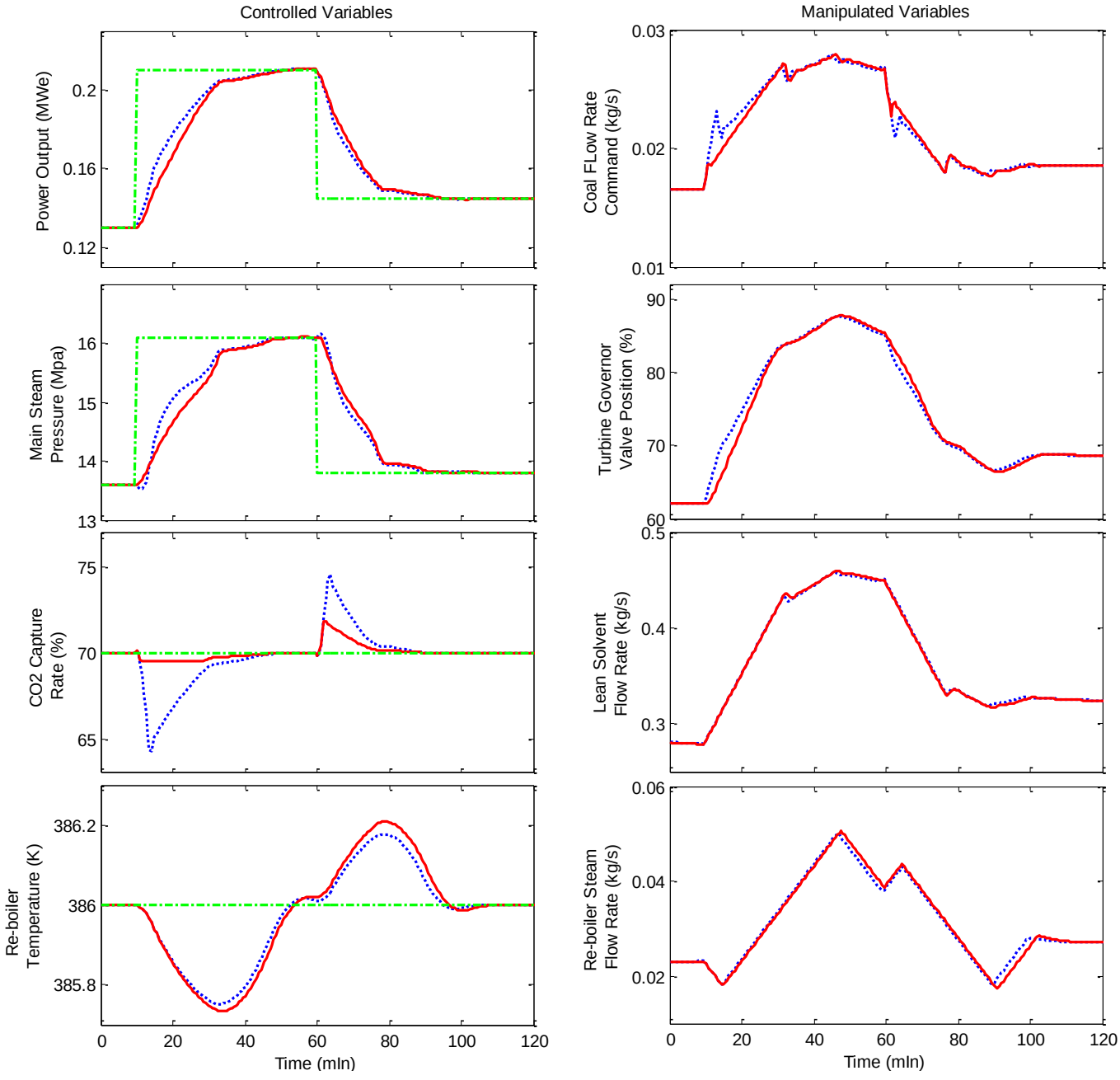

Fig. 8. Performance of the integrated CFPP-PCC system in Case 3: left column: controlled variables; right column: manipulated variables (solid in red: proposed centralized MPC under strict carbon capture mode; dotted in blue: proposed centralized MPC under normal operating mode; dot-dashed in green: reference).

Case 3: Finally, a simulation was designed to demonstrate the control performance of the proposed centralized MPC under strict CO_2 capture requirements. We suppose that in the beginning of the simulation, the CFPP-PCC system is operating at 0.13MWe power output, 13.60MPa main steam pressure, 70% CO_2 capture rate and 386K re-boiler temperature condition. At t=10min and t=60min, the power set-point changes to 0.21MWe and 0.145MWe, respectively, according to the scheduling instructions. While changing the power load, the CO_2 capture rate is expected to be controlled closely around 70% and no less than 69.5%, due to the strict environmental policies and regulations. The main steam pressure set-point changes to 16.10 MPa and 13.80MPa corresponding to the power set-point changes under the sliding pressure mode, and the re-boiler temperature set-point remains at 386K.

The proposed centralized MPC under strict carbon capture mode is used to meet the operation requirement. The weighting matrix Q_0 and R_0 are changed to Q_0=diag(15000, 2, 10000, 100), R_0=diag(4000, 1, 5, 25), in which the weighting values corresponding to the CO_2 capture rate and coal flow rate command are doubled compared with those under the normal operating mode. In addition, $y_{\min}^{capture\_rate}$ is set as 69.5% and the weighting matrix S_f is set as S_f=diag(500000) to give additional penalty when the capture rate is lower than 69.5%. The same centralized MPC under normal operating mode is used for comparison. The simulation results are shown in Fig. 8.

At t=10min, when the power load set-point is raised, the CFPP-PCC plant quickly increase the coal flow rate command and turbine governor valve to increase the power load, the re-boiler steam flow rate is even declined to speed up the load changing rate. The increase of coal flow rate will cause the increase of flue-gas flow rate and sharply drops the CO_2 capture rate. Therefore, the lean solvent flow rate is increased at this stage to compensate the significant decrease of capture rate. However, the effect of lean solvent flow rate on capture rate regulation is only temporary as shown in Fig. 4, and the combined influence of lean solvent, re-boiler steam and flue-gas flow rates will cause the re-boiler temperature to drop rapidly. For this reason, the rising speed of coal flow rate command is slowed down soon to alleviate the influence of flue-gas flow rate on the CO_2 capture rate, and the re-boiler steam flow rate increases to limit the further reduction of the capture rate. It can be observed that the CO_2 capture rate is controlled tightly around 70% point and the lowest value is 69.5% during the power load variation. The re-boiler temperature continues to drop to 385.73K and then gradually returns to the set value. The power and pressure tracking speed is apparently slowed down to meet the capture rate control requirement. About 30 min is taken for them to approach the desired set-points.

For the process of power load decrease, since the decrease of coal mass flow rate will rise the CO_2 capture rate, the constraint and penalty for the capture rate control are not active during the regulation. Thus, the deviation of the capture rate is slightly larger, which is up to 1.7% and still not far away from the 70% set point.

Regarding the proposed centralized MPC under normal operating mode, the actions of lean solvent flow rate and re-boiler steam flow rate are almost the same to those under the strict carbon capture mode. However, in order to balance the power load tracking and CO_2 capture rate control performance, the rising rates of coal flow rate command and turbine governor valve are faster. The increasing speed of power load is thus significantly improved at the early stage of regulation, nevertheless, the fluctuation of capture rate is also increased, which may not meet the operating specification.

The three simulation studies demonstrate the superiority of the proposed centralized MPC approach in achieving a flexible operation of the integrated CFPP-PCC unit. By selecting different modes according to the operating requirements, the centralized MPC can make full use of the integrated CFPP-PCC system's characteristics in power generation and CO_2 emission reduction.

5. Conclusion

This paper develops dynamic models for the integrated CFPP-PCC plant. Step response tests are carried out on the model to investigate the dynamic behavior of the two systems and the interactions among variables in them. It is shown that, the steam flow rate to PCC re-boiler can change the CFPP power output rapidly and the CFPP coal mass flow rate will change the flue-gas flow rate and bring in significant impact on the operation of the PCC unit. Therefore, the independent control of CFPP and PCC systems is not capable of coordinating the two systems and achieving a satisfactory performance for the operation of the integrated CFPP-PCC plant.

For this reason, a centralized MPC is designed for key variables of the CFPP-PCC plant based on the investigation of how

strongly the two systems are linked together. The interactions between the key variables can thus be fully estimated and utilized. To better coordinate the operation of the CFPP and PCC systems, three operating modes are considered for the centralized MPC according to different operating requirements, which are the normal operating mode, the rapid power ramping mode and the strict carbon capture mode. The centralized MPC can greatly benefit the flexible operation of the integrated system and better exerts its powerful functions in power generation and CO_2 reduction.

Acknowledgements

The authors would like to acknowledge the National Natural Science Foundation of China (NSFC) under Grant 51506029, the Natural Science Foundation of Jiangsu Province, China under Grant BK20150631, China Postdoctoral Science Foundation, EU FP7 International Staff Research Exchange Scheme on power plant and carbon capture (Ref: PIRSES-GA-2013-612230).

References

[1] EU, Global and European sea-level rise, from http://www.eea.europa.eu/data-and-maps/indicators/sea-level-rise-2/assessment, Accessed on 18th May 2018

[2] IEA, Electricity information 2017, IEA Publications, Aug. 2017.

[3] IEA, The potential for carbon capture and storage in China, published on 17th Jan. 2017, from http://www.iea.org/newsroom/news/2017/january/the-potential-for-carbon-capture-and-storage-in-china.html, Accessed on 18th May 2018.

[4] M. Wilson, P. Tontiwachwuthikul, A. Chakma, R. Idem, A. Veawab, A. Aroonwilas, D. Gelowitz, J. Barrie, and C. Mariz. Test results from a CO2 extraction pilot plant at boundary dam coal-fired power station. Energy, vol. 29, pp. 1259-1267, 2004.

[5] IEEE Spectrum, Construction start on world's largest post-combustion carbon capture project, published on 17th Jul. 2014, from https://spectrum.ieee.org/energywise/green-tech/clean-coal/construction-starts-on-worlds-largest-postcombustion-carbon-capture-project, Accessed on 23th Jul. 2018.

[6] P. Galindo Cifre, K. Brechtel, S. Hoch, H. García, N. Asprion, H. Hasse, and G. Scheffknecht. Integration of a chemical process model in a power plant modelling tool for the simulation of an amine based CO2 scrubber. Fuel, vol. 88, pp. 2481-2488, 2009.

[7] A. Aroonwilas and A. Veawab. Integration of CO2 capture unit using single- and blended-amines into supercritical coal-fired power plants: Implications for emission and energy management. International Journal of Greenhouse Gas Control, vol. 1, pp. 143-150, 2007.

[8] T. Sanpasertparnich, R. Idem, I. Bolea, D. Montigny, and P. Tontiwachwuthikul. Integration of post-combustion capture and storage into a pulverized coal-fired power plant. International Journal of Greenhouse Gas Control, vol. 4, pp. 499-510, 2010.

[9] S. Oh, S. Yun, and J. Kim. Process integration and design for maximizing energy efficiency of a coal-fired power plant integrated with amine-based CO2 capture process. Applied Energy, vol. 216, pp. 311-322, 2018.

[10] M. Pan, F. Aziz, B. Li, S. Perry, N. Zhang, I. Bulatov, and R. Smith. Application of optimal design methodologies in retrofitting natural gas combined cycle power plants with CO2 capture. Applied Energy, vol. 161, pp. 695-706, 2016.

[11] D. Wang, S. Li, F. Liu, L. Gao, and J. Sui. Post combustion CO2 capture in power plant using low temperature steam upgraded by double absorption heat transformer. Applied Energy, in press, 2017.

[12] M. Lucquiaud, H. Chalmers, and J. Gibbins. Capture-ready supercritical coal-fired power plants and flexible post-combustion CO2 capture. Energy Procedia, vol. 1, pp.1411-1418, 2009.

[13] E. S. Fernandez, M. Sanchez del Rio, H. Chalmers, P. Khakharia, E. L. V. Goetheer, J. Gibbins, and M. Lucquiaud. Operational flexibility options in power plants with integrated post-combustion capture. International Journal of Greenhouse Gas Control, vol. 48, pp. 275–289, 2016.

[14] J. Rodriguez, A. Andrade, A. Lawal, N. Samsatli, S. Calado, T. Lafitte, J. Fuentes, and C. Pantelides. An integrated framework for the dynamic modelling of solvent-based CO_2 capture processes. Energy Procedia vol.63, pp. 1206-1217, 2014.

[15] E. Mechleri, A. Lawal, A. Ramos, J. Davison, and N. Mac Dowell. Process control strategies for flexible operation of post-combustion CO_2 capture plants. International Journal of Greenhouse Gas Control, vol. 57, pp. 14-25, 2017.

[16] F. Li, J. Zhang, E. Oko, and M. Wang. Modelling of a post-combustion CO_2 capture process using neural networks. Fuel, vol. 151, pp. 156-163, 2015.

[17] N. A. Manaf, A. Cousins, P. Feron, and A. Abbas. Dynamic modelling. Identification and preliminary control analysis of an amine-based post-combustion CO_2 capture pilot plant. Journal of Cleaner Production, vol. 113, pp. 635-653, 2016.

[18] R. Faber, M. Kopcke, O. Biede, J. N. Knudsen, and J. Andersen. Open-loop responses for the MEA post combustion capture process: Experimental results from the Esbjerg pilot plant. Energy Procedia, vol. 4, pp. 1427-1434, 2011.

[19] M. Bui, I. Gunawan, V. Verheyen, P. Feron, and E. Meuleman. Flexible operation of CSIRO's post-combustion CO_2 capture pilot plant at the AGL Loy Yang power station. International Journal of Greenhouse Gas Control, vol. 48, pp. 188-203, 2016.

[20] X. Wu, J. Shen, Y. Li, M. Wang, A. Lawal, and K. Y. Lee. Nonlinear dynamic analysis and control design of a solvent-based post-combustion CO2 capture process. Computers & Chemical Engineering, vol. 115, pp. 397-406, 2018.

[21] A. Lawal, M. Wang, P. Stephenson, G. Koumpouras, and H. Yeung. Dynamic modelling and analysis of post-combustion CO_2 chemical absorption process for coal-fired power plants. Fuel, vol. 89, pp. 2791-2801, 2010.

[22] Y. Lin, T. Pan, D. Wong, S. Jang, Y. Chi, and C. Yeh. Plantwide control of CO_2 capture by absorption and stripping using monoethanolamine solution. Ind Eng Chem Res, vol. 50, pp. 1338-1345, 2011.

[23] M. Panahi and S. Skogestad. Economically efficient operation of CO_2 capturing process part I: self-optimizing procedure for selecting the best controlled variables. Chemical Engineering and Processing: Process Intensification, vol. 50, no.3, pp. 247-253, 2011.

[24] T. Nittaya, P. L. Douglas, E. Croiset, and L. A. Ricardez-Sandoval. Dynamic modelling and control of MEA absorption processes for CO_2 capture from power plants. Fuel, vol. 116, pp. 672-691,2014.

[25] Q. Zhang, R. Turton, and D. Bhattacharyya. Development of Model and Model-Predictive Control of an MEA-Based Post combustion CO_2 Capture Process. Industrial & Engineering Chemistry Research, vol. 55, pp. 1292-1308, 2016.

[26] X. Wu, J. Shen, Y. Li, M. Wang, and A. Lawal. Flexible operation of post-combustion solvent-based carbon capture for coal-fired power plants using multi-model predictive control: a simulation study. Fuel, vol. 220, pp.931-941, 2018.

[27] A. Cormos, M. Vasile, and M. Cristea. Flexible operation of CO_2 capture processes integrated with power plant using advanced control techniques. 12th International Symposium on Process Systems Engineering and 25th European Symposium on Computer Aided Process Engineering, Copenhagen, Denmark, May 31-Jun 4, 2015.

[28] M. T. Luu, N. A. Manaf, and A. Abbas, Dynamic modelling and control strategies for flexible operation of amine-based post-combustion CO2 capture systems, International Journal of Greenhouse Gas Control. vol. 39, pp. 377-389, 2015.

[29] A. Lawal, M. Wang, P. Stephenson, and H. Yeung. Dynamic modelling of CO_2 absorption for post combustion capture in coal-fired power plants. Fuel, vol. 88, pp. 2455-2462, 2009.

[30] S. Posch and M. Haider. Dynamic modelling of CO_2 absorption from coal-fired power plants into an aqueous monoethanolamine solution. Chem Eng Res Des, vol. 91, pp. 977-987, 2013.

[31] N. A. Manaf, A. Qadir and A. Abbas. The hybrid MPC-MINLP algorithm for optimal operation of coal-fired power plants with solvent based post-combustion CO_2 capture. Petroleum, vol. 3, pp. 155-166, 2017.

[32] N. Mac Dowell and N. Shah. The multi-period optimisation of an amine-based CO_2 capture process integrated with a super-critical coal-fired power station for flexible operation. Computers and Chemical Engineering, vol. 74, pp. 169-183, 2015.

[33] A. Lawal, M. Wang, P. Stephenson, and O. Obi. Demonstrating full-scale post-combustion CO_2 capture for coal-fired power plants through dynamic modelling and simulation. Fuel, vol. 101, pp. 115-128, 2012.

[34] A. K. Olaleye, E. Oko, M. Wang, and G. Kelsall. Dynamic modelling and analysis of supercritical coal-fired power plant integrated with post-combustion CO2 capture. Clean Coal Technology and Sustainable Development: Proceedings of the 8th International Symposium on Coal Combustion, pp. 359-363, Springer Science+ Business Media Singapore and Tsinghua University Press, Singapore, 2016.

[35] E. R. Dugas. Pilot plant study of carbon dioxide capture by aqueous monoethanolamine. M.S.E. Thesis, University of Texas at Austin; 2006.

[36] X. Wu, J. Shen, Y. Li, and K. Y. Lee. Steam power plant configuration, design and control. WIREs Energy Environ, vol. 4, no. 6, pp. 537-563, Nov-Dec. 2015.

[37] J. Liu, S. Yan, D. Zeng, Y. Hu, and Y. Lv. A dynamic model used for controller design of a coal fired once-through boiler-turbine unit. Energy, vol. 93, pp. 2069–2078. 2015.

[38] L. Tian, D. Zeng, J. Liu, and Z. Zhao. A simplified nonlinear dynamic model of 330MW unit. Proceedings of the CSEE, vol. 24, No. 8, pp. 180-184, 2004 (in Chinese).

[39] G. Feng. A survey on analysis and design of model-based fuzzy control systems. IEEE Transactions on Fuzzy Systems, vol. 14, no. 5, pp. 676-697, 2006.

[40] X. Wu, J. Shen, Y. Li, and K. Y. Lee. Data-driven modeling and predictive control for boiler-turbine unit. IEEE Trans. on Energy Conversion, vol. 28, No. 3, pp 470-481, Sep, 2013.